Chemical Science

ROYAL SOCIETY OF CHEMISTRY

EDGE ARTICLE

View Article Online
View Journal | View Issue

Cite this: *Chem. Sci.*, 2024, **15**, 15873

All publication charges for this article have been paid for by the Royal Society of Chemistry

Received 3rd July 2024
Accepted 28th August 2024

DOI: 10.1039/d4sc04411h

rsc.li/chemical-science

Snapshot of cyclooctyne ring-opening to a tethered alkylidene cyclic polymer catalyst†

Javier M. Hurst,[a] Rinku Yadav,[a] Parker T. Boeck,[ab] Ion Ghiviriga,[ab] ChristiAnna L. Brantley,[ab] Łukasz Dobrzycki[ab] and Adam S. Veige *[ab]

Cyclooctyne reacts with the trianionic pincer ligand supported alkylidyne [^{t}BuOCO]WCC(CH$_3$)$_3$(THF)$_2$ (**1**) to yield tungstacyclopropene (**3**) and tungstacyclopentadiene (**4**) complexes. The ratio of **3** and **4** in the reaction mixture depends on the stoichiometry of the reaction. The maximum concentration of **3** occurs with one equiv. of cyclooctyne and **4** is the exclusive product of the reaction above three equivalents. Both complexes **3** and **4** convert to the cyclooctyne ring-opened product **5** upon heating. While the conversion of **4** to **5** is accompanied by formation of polycyclooctyne as a white precipitate during the reaction, conversion of **3** to **5** is homogeneous. Exhibiting Ring Expansion Polymerization (REP), complexes **4** and **5** initiate the polymerization of phenylacetylene to generate cyclic poly(phenylacetylene) (c-PPA).

Cyclic polymers do not have chain ends[1] and have notably different physical, biological, and chemical properties compared to their linear analogues with similar molar mass. Cyclic polymers exhibit higher glass transition temperature (T_g),[2–4] smaller radii of gyration,[5,6] lower intrinsic viscosity,[7,8] and higher thermal stability.[9,10] Changing polymer topology imparts a significant difference in biological properties. For instance, cyclic polymers exhibit higher tumor penetration ability,[11–13] cytotoxicity,[14] and nucleic acid delivery.[12] When grafted on a surface, cyclic polymers have lower friction coefficients,[15,16] smaller nanostructure domain spacing,[17] and higher surface annealing rates.[18] Increased nucleation density and crystallization rates were measured for cyclic polymers.[19] Enhanced conjugation in cyclic polymers also affects photophysical properties including higher fluorescence emission and excited state-lifetime,[20] and higher refractive index.[21] Conventional synthetic routes to obtain cyclic polymers rely on coupling chain ends of linear polymers.[22,23] Coupling chain ends requires multiple synthetic steps, is laborious, and often requires dilute conditions though improved approaches are emerging.[24–26]

In 2016, we reported the trianionic pincer[27–30] alkylidyne complex **1** (ref. 31–33) transforms to the tethered tungsten alkylidene complex **2** (Scheme 1) when treated with 4,4-dimethyl-but-1-yne.[34] Complex **2** rapidly initiates ring expansion polymerization (REP) of alkynes to generate cyclic polyenes in excellent yields with diverse functional groups.[35]

The REP mechanism, introduced by Lee and Kricheldorf using a dibutyltin catalyst in 1995,[36] involves repeated monomer insertions into a growing ring.[37–41] New REP initiators and an ever-expanding list of monomers are appearing in the literature.[37,42] The initial proposal for ring formation with complex **2** was published in 2016 (Fig. 1). In that work, because complex **2** does not undergo metathesis with preformed cyclic polyphenylacetylene, the tethered alkylidene was not invoked as the site of ring expansion and only played the role of ancillary ligand. Instead, the mechanism implied sequential insertions to grow a metallacycle where an intermediate **2b** (Fig. 1) forms and then eliminates the cyclic polymer in a reductive elimination step.[34] Support at the time, and since, for **2b** as an intermediate in the polymerization came from the isolation of several ring expanded metallacyclopentadiene species.[43–45] The extreme rates (1.8×10^8 g mol^{-1} h^{-1})[46] recorded for polymerizations initiated by **1** and **2** make it difficult to ascertain the mechanism of alkyne REP.

In this work, a snapshot of cyclooctyne (CyO) ring-opening across the tethered alkylidene of **2** provides new insight into

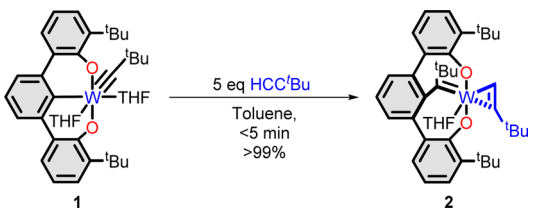

Scheme 1 Reported synthesis of REP initiator **2**.

[a]*University of Florida, Department of Chemistry, Center for Catalysis, P.O. Box 117200, Gainesville, FL, 32611, USA. E-mail: veige@chem.ufl.edu*

[b]*University of Florida, Department of Chemistry, George and Josephine Butler Polymer Research Laboratory, Center for Macromolecular Sciences and Engineering, Gainesville, FL, 32611, USA*

† CCDC 2360874–2360876. For crystallographic data in CIF or other electronic format see DOI: https://doi.org/10.1039/d4sc04411h

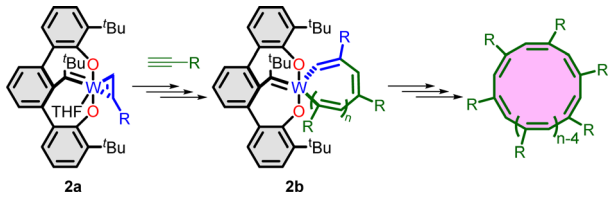

Fig. 1 Original proposed REP pathway for the synthesis of cyclic polyenes.

the possible mechanism and suggests the tethered alkylidene may participate in the REP mechanism after all. Complex **2** rapidly polymerizes small non-coordinating monosubstituted alkynes but does not react with bulky or disubstituted alkynes at room temperature.[35] A simple strategy to trap an intermediate in such a case is to hinder propagation with an appropriately bulky substrate. Metallacycopentadiene trapping events employ a similar strategy; however, those reactions require elevated temperatures (75 °C) to induce insertion.[43] It is possible to miss reactive intermediates at high temperatures. Ideally, the reaction probe uses relatively lower temperatures to observe elusive intermediates. CyO is disubstituted, thus bulky enough to inhibit propagation but also significantly strained, making initial insertions favorable. Therefore, CyO was chosen for this study resulting in the first isolation of a complex featuring a ring opened CyO.

Treating a dark red benzene solution of **1** with CyO results in an immediate color change to amber and finally to olive green. The reaction between **1** and CyO simultaneously yields tungstacyclopropene (**3**) and tungstacyclopentadiene (**4**) tethered alkylidene complexes (Scheme 2). Complex **4** forms exclusively when combining 2.5 (or above) equivalents of CyO and **1**. However, **3** always coexists with **4** in solution even at substoichiometric additions. Table 1 and Fig. 2 depict the relationship between the relative amounts of complexes **1**, **3**, and **4** that form in benzene solution *vs.* equiv. of CyO added; the maximum concentration of **3** occurs with 1 equiv. It is important to notice that insertion of CyO in **1** is rapid leading to a mixture of either **3** and **4**, or solely **4**. Therefore, it is impossible to exclusively obtain **3** from **1**. Exposing **1** to CyO in the presence of excess THF does favor the formation of **3**. For example, addition of one equiv. of CyO in the presence of 10 equiv. of THF in benzene results in a relative ratio of 7 : 8 : 2 of complexes **1** : **3** : **4**, respectively. Performing the same reaction with THF as solvent does not improve the outcome in favor of **3**.

Complex **3** co-crystallizes as light orange crystals with dark olive green crystals of **4** from a concentrated Et_2O solution of **1** : **3** : **4** in ratio 7 : 8 : 2, respectively, within several days at −30 °C. Consequently, it is not possible to obtain pure **3** in large quantities. Single crystals of **4** deposit exclusively from a concentrated Et_2O solution of **4** at −30 °C overnight. Single crystal X-ray diffraction experiments provide unambiguous assignment of **3** as a tungstacyclopropene and **4** as a tungstacyclopentadiene (Fig. 3); Table 2 lists selected bond lengths and angles. Both **3** and **4** are pseudo-C_s symmetric with the plane of symmetry bisecting the OCO pincer ligand and W=C bond.

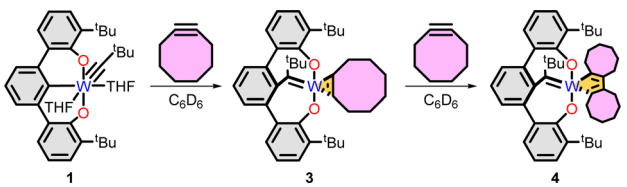

Scheme 2 Synthesis of complexes **3** and **4**.

Table 1 Yield (%) of **1**, **3**, and **4** *vs.* CyO equivalents

CyO	1	3	4
0.25	83	11	6
0.58	60	22	18
1.11	27	35	38
1.52	13	34	53
1.97	0	3	97
2.50	0	0	100

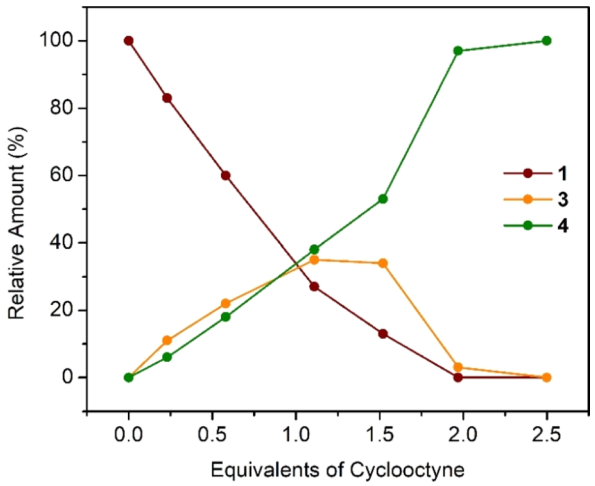

Fig. 2 Yield (%) of **1**, **3**, and **4** *vs.* CyO equivalents.

Complex **3** consists of a formally W(VI) ion that diverges from a conventional polyhedral geometry. The W1–C27 bond length of 1.904(2) Å resembles previously reported W(VI) alkylidene complexes; for example, **2** has a W1–C27 bond length of 1.9021(19) Å.[34] The W1–C32 (2.043(2) Å), W1–C39 (2.027(2) Å) and C32–C39 (1.309(4) Å) bond lengths are statistically similar to reported η^2-bound W-alkyne complexes (Table S4†).[34,47–50] An elongated W1–O3 bond length of 2.3003(17) Å implies that the alkylidene exerts a strong *trans* influence on bound THF. Solution state NMR studies indicate **3** retains C_s symmetry in solution. The ^{1}H NMR spectrum of **3** in benzene-d_6 exhibits two singlets at 0.89 and 1.26 ppm in a relative integration ratio of 1 : 2 for the alkylidene-^{t}Bu and aryl-^{t}Bu protons, respectively. A ^{13}C $\{^1H\}$ spectrum of **3** reveals a resonance at 263.4 ppm for the alkylidene carbon.

For complex **4**, an Addison parameter value τ of 0.53 suggests that the ligand geometry around the formally W(VI) ion is

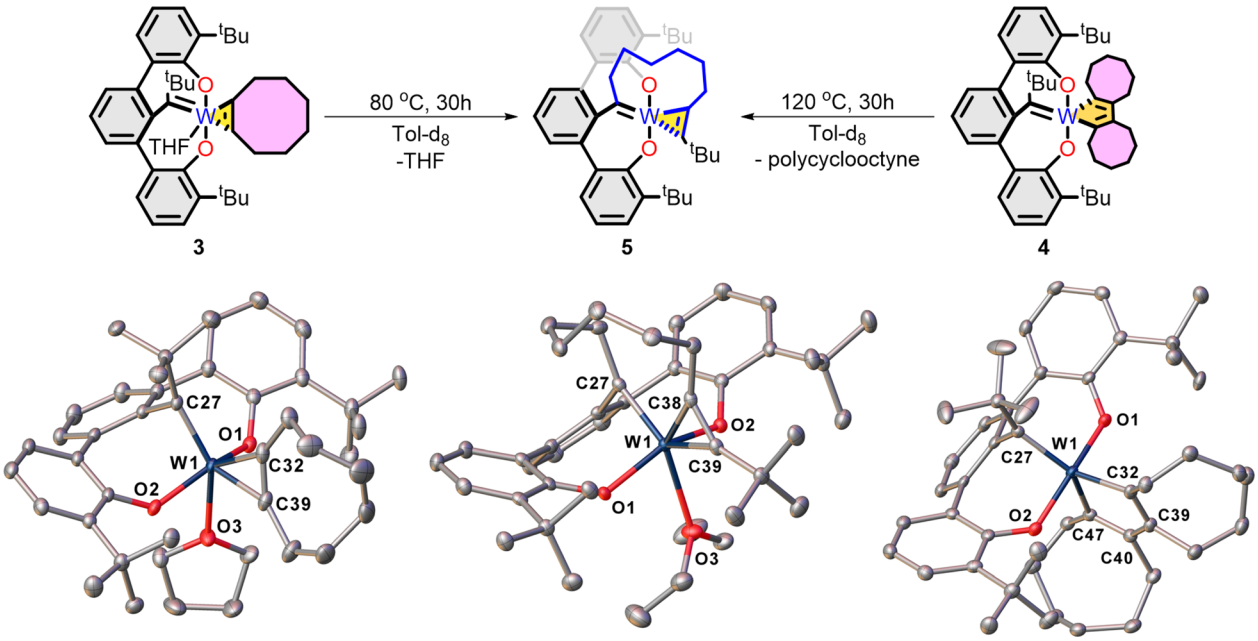

Fig. 3 Synthesis of complex 5 and crystal structures of 3, 4, and 5.

Table 2 Selected bond lengths (Å) and angles (°) for 3, 4, 5

	3	4	5
W1–C27	1.904(2)	1.908(6)	1.895(2)
W1–C32	2.043(2)	2.071(9)	—
W1–C38	—	—	2.022(2)
W1–C39	2.027(2)	—	2.037(2)
C32–C39	1.309(4)	1.381(6)	—
C38–C39	—	—	1.316(3)

between square pyramidal and trigonal bipyramidal.[51] The W1–C32 (2.071(9) Å), W1–C47 (2.080(7) Å), C32–C39 (1.381(6) Å) and C40–C47 (1.370(6) Å) bond lengths in **4** are all similar to reported tungstacyclopentadiene complexes.[43,52–54] Differences in the bond lengths and angles of the metallacyclopentadiene ring are likely attributable to the ring strain of the CyO substituents; however, the alkylidene is statistically the same bond length as that of a previously reported metallacyclopentadiene complex (Table S5†). Complex **4** also retains C_s symmetry in solution. The ^{1}H NMR spectrum of **4** in benzene-d_6 exhibits two distinct singlets at 0.98 ppm and 1.55 ppm with a relative integration of 1 : 2 for the alkylidene-^{t}Bu and pincer-^{t}Bu protons, respectively. A resonance for the alkylidene carbon appears at 311.3 ppm in the ^{13}C NMR spectrum. Although, it is unusual for an alkylidene carbon to resonate so far downfield, a similar signal was observed for other tungstacyclopentadienes.[43]

Complexes **3** and **4** form as the result of a migratory insertion of the alkylidyne carbon into the tungsten arene bond of the pincer ligand. The migratory insertion event is a distinctive property of **1** and occurs with various substrates with high rates.[34,43,50,55–59] The ring strain of cyclooctyne (~18 kcal mol^{-1})[60–63] must play a role in the swift insertion to give **4** since disubstituted alkynes require heating to induce metallacylopentadiene formation.

According to the originally proposed REP mechanism (Fig. 1), successive addition of alkyne monomers in the metallacyclopropene ring generates a cyclic polymer. Perhaps signifying an alternative mechanism, isolating a metallacycloheptatriene by adding additional alkyne equivalents was not successful. However, **4** initiates the polymerization of phenylacetylene even at −30 °C. Monitoring a 1 : 1 (**4** : phenylacetylene) reaction by ^{1}H NMR spectroscopy reveals the alkyne directly converts into polymer without showing any detectable signals of an intermediate species (Fig. S12†). As is typical for these polymerizations a significant amount of unreacted **4** remains during the polymerization, indicative of slow initiation and rapid propagation kinetics. Exposing **4** to excess CyO leads to an insoluble white cyclooctyne polymer. Consistent with reported literature, polycyclooctyne is insoluble in THF, toluene, *o*-dichlorobenzene, and other common organic solvents consequently preventing its characterization.[64,65] The IR spectrum of the white precipitate does not exhibit a C≡C stretch (Fig. S39†). Instead, it exhibits a C=C stretch at 1440 cm^{-1} indicating the conversion of CyO to poly-CyO.

Providing insight into the role of the tethered alkylidene and its ability to engage in metathesis with alkynes, heating **3** at 80 °C for 30 h provides the cyclooctyne ring opened product **5** (Fig. 3). A similar transformation occurs in the case of **4** as well, but it is slower and requires 120 °C to complete in the same time frame. The color of the solution changes from orange (**3**) or olive green (**4**) to red orange (**5**) during these transformations. The formation of **5** from **3** and **4** at elevated temperatures indicates that **5** is the thermodynamic product from the overall reaction between **1** and CyO. Conversion of **3** to **5** occurs homogeneously, whereas conversion of **4** to **5** is accompanied

with the formation of a white precipitate. The white precipitate is insoluble in common organic solvents leading to the conclusion that it is also polycyclooctyne, that results from shedding one equivalent of cyclooctyne.

Single crystals suitable for X-ray data collection accumulate from a concentrated Et_2O solution of **5** at −30 °C within several days. Fig. 3 depicts the solid-state structure of **5**. Similar to **3**, **5** also contains a tungstacyclopropene, belongs to C_s symmetry in the solid-state, and exhibits analogous structural features (Table 2). A noticeable and unexpected structural difference among **3**, **4**, and **5** is a contracted alkylidene bond in **5** (1.895(2) Å), presumably due to the tether between the alkylidene and η^2-bound alkyne. Additional evidence suggesting the tether alters the alkylidene is the bond angle between the alkylidene and the adjacent carbon of the bound alkyne is considerably smaller for **5** by 5.64(14)°.

The coordinated Et_2O, from solvent, is weakly bound in **5** (2.300 (17) Å) akin to THF in **3** (2.390 (17) Å). Key to the structure is the unambiguous presence of a tether between the alkylidene and the η^2-bound alkyne. Evidence of the tether in solution comes from ^{1}H, ^{13}C, HSQC, HMBC, and COSY NMR data (see ESI† for spectra).

Akin to their parent complexes **1**, **4** and **5** polymerize phenylacetylene. In a typical polymerization reaction, the required amount of a stock solution of pure initiator **4** or **5** was added to a stirring solution of freshly dried and distilled phenylacetylene in toluene. As the reaction stirs, the color of the solution changes from green to deep red. Reactions using **4** as the catalyst were stirred for 12 h, while reactions with **5** were stirred for 3 h (Fig. 4, Table 3). Adding the reaction mixture dropwise into oxygen free methanol precipitates the polymer. Precipitation of polyenes requires oxygen free methanol as conjugated polyenes degrade *via* oxidation.[35] The polymerization experiments were conducted in triplicate for **4** and **5**, (see ESI†).

For comparison, linear polyphenylacetylene (l-PPA) was prepared according to literature procedures using (acetylacetonato)(1,5-cyclooctadiene)rhodium(I) [acac(Rh(I)cod)]. Importantly, PPA samples prepared with **4**, **5**, and [acac(Rh(I)cod)][66,67] contain >90% *cis* double bonds, as determined by NMR spectroscopy (Fig. S30–S35†).

Cyclic polymers exhibit distinct physical properties compared to linear polymers of comparable molecular weight, enabling the determination of their topology by size exclusion chromatography (SEC) coupled to viscometer measurements and static light scattering techniques.[68–71] Fig. 5 depicts a plot of the log of molar mass *versus* retention time for l-PPA and c-PPA synthesized by **4**. It is clear from the graph that PPA synthesized by **4** elutes later than l-PPA at a given molar mass, consistent with a cyclic topology. Fig. 6 depicts a plot of root mean square radii of gyration *vs.* log of molar mass. Again, it is apparent from the plot that the radius of gyration of PPA produced from complex **4** is smaller than a known linear analogue at a given molar mass.[9] PPA synthesized using **5** also has the same relationship to the linear version indicating a cyclic topology (Fig. S37 and S38†).

Table 3 GPC data of *c*-PPA obtained using **4** and **5** as catalysts

	4	**5**
M_n[a,b]	279 kDa	337 kDa
M_w[a,b]	368 kDa	429 kDa
$Đ$[a,b]	1.32	1.27
Yield[a]	49%	22%

[a] Values are an average of three from triplicate experiments. [b] Measured using GPC (50 °C, DMAc, dLS detection).

Discussion

Cyclooctyne instantaneously reacts with **1** at room temperature. The outcome of the reaction is heavily dependent on the stoichiometry. Surprisingly, the expected tungstacyclopropene **3**, is not a major product of the reaction especially at higher equivalents of cyclooctyne. Unlike previously reported tungstacyclopropene complexes,[43] **3** does not establish a detectable equilibrium with its metathesis isomer **5** at ambient temperature. For example, alkylidyne **1** reacts with 1 equiv. of 1-phenyl-1-propyne to yield two metathesis isomers, **6a** and **6b** in a 1 : 2 ratio respectively (Scheme 3).[43] Presumably, isomerization proceeds through a traditional metallacylcobutadiene intermediate by cleavage of the C–C bond to the pincer backbone.

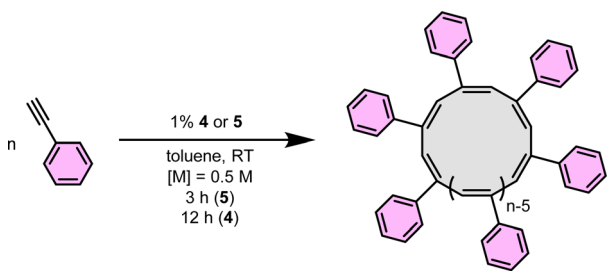

Fig. 4 Polymerization of phenylacetylene to generate cyclic polyphenylacetylene (c-PPA) with **4** and **5** as catalysts.

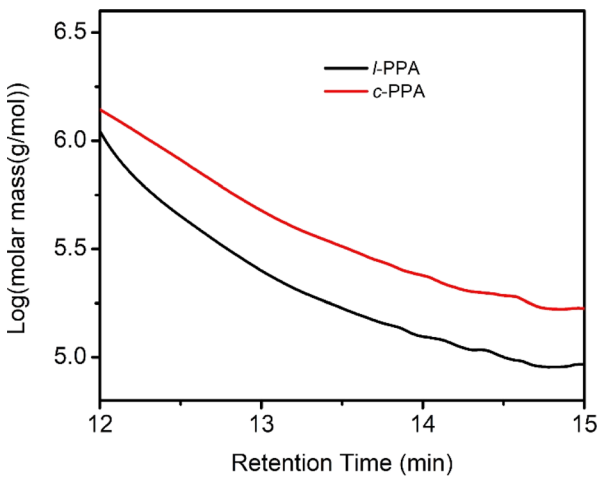

Fig. 5 Log (molar mass(g mol^{-1})) *versus* retention time graph for *c*-PPA (red) synthesized by **4** and linear polyphenylacetylene (l-PPA, black).

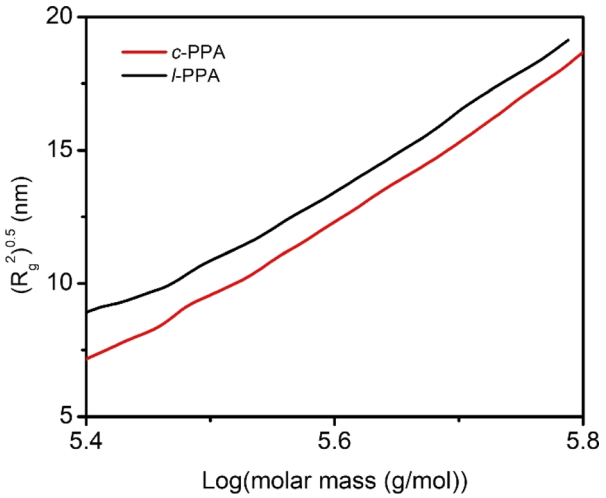

Fig. 6 Root mean square radii of gyration *versus* Log (molar mass(g mol^{-1})) graph for *c*-PPA (red) synthesized by **4** and linear poly-phenylacetylene (l-PPA, black).

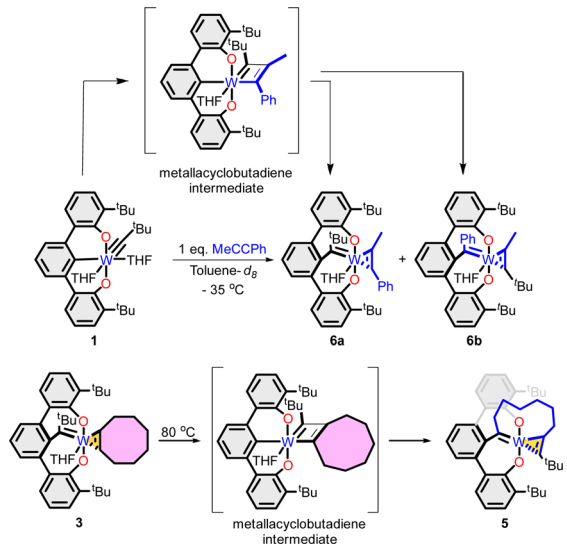

Scheme 3 Proposed role of metallacyclobutadiene in tethered alkylidene formation.

Published examples indicate the C–C bond cleavage is surprisingly facile in this pincer framework and is a hallmark of the high reactivity. For **3**, due to the cyclic nature of CyO, forming a metallacyclobutadiene intermediate followed by metathesis yields the ring opened product as the tethered alkylidene **5**.

In an alternative route, heating **4** also produces the tethered alkylidene **5** presumably by first expelling an equiv. of cyclooctyne to revert to **3** followed by metathesis as in Scheme 3. Monitoring the conversion of **4** to **5** *via* ^{1}H NMR spectroscopy does not reveal any detectable signals or buildup of **3**.

Conclusions

Alkylidyne **1** is an initiator for the polymerization of alkynes to give cyclic polymers by first transforming into tethered alkylidene with a bound alkyne according to Scheme 1. A previously proposed mechanism[34] neglected the potential role of the tethered alkylidene in the propagation of the growing ring. The main conclusion from this work is the isolation of and existence of **5** demonstrates that the tether is a reasonable composition for possible active species in both ring expansion metathesis polymerization (REMP) of alkynes and cyclic alkenes such as norbornene. Complexes **4** and **5** polymerize phenylacetylene to give cyclic polymers. Though much work remains to elucidate other intermediates in the polymerization, isolation of a tethered alkylidene within **5**, at least from a compositional standpoint, offers new insight. Complex **5** is also a snapshot of a ring-opened cyclic alkyne *via* metathesis, an elusive intermediate until now.

Data availability

The data supporting this article have been included as part of the ESI.†

Author contributions

JMH carried out all experiments. CLB, RY, and LD collected and refined the X-ray data. IG assisted in NMR characterizations. PTB characterized the polymer samples. RY and JMH drafted the manuscript. RY, JMH, ASV, and PTB revised the manuscript. ASV and RY supervised the work. All authors have given approval to the final version of the manuscript.

Conflicts of interest

ASV has an equity position in Oboro Labs Inc.

Acknowledgements

This material is based upon work supported by the National Science Foundation CHE-2154377 (A. S. V.). The GC/EI-MS instrument is funded by NIH S10 OD021758-01A1. LD acknowledges the NSF (CHE-1828064) and UF for the purchase of X-ray equipment.

Notes and references

1 Z. Jia and M. J. Monteiro, *J. Polym. Sci., Part A: Polym. Chem.*, 2012, **50**, 2085–2097.
2 D. J. Bannister and J. A. Semlyen, *Polymer*, 1981, **22**, 377–381.
3 S. J. Clarson, K. Dodgson and J. A. Semlyen, *Polymer*, 1985, **26**, 930–934.
4 L. Gao, J. Oh, Y. Tu, T. Chang and C. Y. Li, *Polymer*, 2019, **170**, 198–203.
5 J. Roovers, *J. Polym. Sci.*, 1985, **23**, 1117–1126.
6 T. E. Gartner, F. M. Haque, A. M. Gomi, S. M. Grayson, M. J. A. Hore and A. Jayaraman, *Macromolecules*, 2019, **52**, 4579–4589.
7 Y. Jeong, Y. Jin, T. Chang, F. Uhlik and J. Roovers, *Macromolecules*, 2017, **50**, 7770–7776.

8 R. Liénard, J. De Winter and O. Coulembier, *J. Polym. Sci.*, 2020, **58**, 1481–1502.
9 B. H. Zimm and W. H. Stockmayer, *J. Chem. Phys.*, 1949, **17**, 1301–1314.
10 R. Zhang, M. M. Billingsley and M. J. Mitchell, *J. Controlled Release*, 2018, **292**, 256–276.
11 C. E. Wang, H. Wei, N. Tan, A. J. Boydston and S. H. Pun, *Biomacromolecules*, 2016, **17**, 69–75.
12 B. Chen, K. Jerger, J. M. J. Fréchet and F. C. Szoka, *J. Controlled Release*, 2009, **140**, 203–209.
13 B. Golba, E. M. Benetti and B. G. De Geest, *Biomaterials*, 2021, **267**, 120468.
14 N. Nasongkia, B. Chen, N. Macaraeg, M. E. Fox, J. M. J. Fréchet and F. C. Szoka, *J. Am. Chem. Soc.*, 2009, **131**, 3842–3843.
15 G. Morgese, L. Trachsel, M. Romio, M. Divandari, S. N. Ramakrishna and E. M. Benetti, *Angew. Chem., Int. Ed.*, 2016, **55**, 15583–15588.
16 A. Patel, T. Cosgrove and J. A. Semlyen, *Polymer*, 1991, **32**, 1313–1317.
17 A. D. Goodson, J. E. Troxler, M. S. Rick, H. S. Ashbaugh and J. N. L. Albert, *Macromolecules*, 2019, **52**, 9389–9397.
18 L. Wang, L. Xu, B. Liu, T. Shi, S. Jiang and L. An, *Soft Matter*, 2017, **13**, 3091–3098.
19 N. Zaldua, R. Liénard, T. Josse, M. Zubitur, A. Mugica, A. Iturrospe, A. Arbe, J. De Winter, O. Coulembier and A. J. Müller, *Macromolecules*, 2018, **51**, 1718–1732.
20 X. Zhu, N. Zhou, Z. Zhang, B. Sun, Y. Yang, J. Zhu and X. Zhu, *Angew. Chem., Int. Ed.*, 2011, **50**, 6615–6618.
21 D. J. Orrah, J. A. Semlyen and S. B. Ross-Murphy, *Polymer*, 1988, **29**, 1455–1458.
22 D. Pasini, *Molecules*, 2013, **18**, 9512–9530.
23 K. Pangilinan and R. Advincula, *Polym. Int.*, 2014, **63**, 803–813.
24 H. R. Kricheldorf, *J. Polym. Sci., Part A: Polym. Chem.*, 2010, **48**, 251–284.
25 M. Kapnistos, M. Lang, D. Vlassopoulos, W. Pyckhout-Hintzen, D. Richter, D. Cho, T. Chang and M. Rubinstein, *Nat. Mater.*, 2008, **7**, 997–1002.
26 W. Lee, H. Lee, H. C. Lee, D. Cho, T. Chang, A. A. Gorbunov and J. Roovers, *Macromolecules*, 2002, **35**, 529–538.
27 J. Koller, S. Sarkar, K. A. Abboud and A. S. Veige, *Organometallics*, 2007, **26**, 5438–5441.
28 S. Sarkar, K. P. McGowan, J. A. Culver, A. R. Carlson, J. Koller, A. J. Peloquin, M. K. Veige, K. A. Abboud and A. S. Veige, *Inorg. Chem.*, 2010, **49**, 5143–5156.
29 S. S. Nadif, M. E. O'Reilly, I. Ghiviriga, K. A. Abboud and A. S. Veige, *Angew. Chem., Int. Ed.*, 2015, **54**, 15138–15142.
30 M. E. O'Reilly and A. S. Veige, *Chem. Soc. Rev.*, 2014, **43**, 6325–6369.
31 S. Sarkar, K. P. McGowan, S. Kuppuswamy, I. Ghiviriga, K. A. Abboud and A. S. Veige, *J. Am. Chem. Soc.*, 2012, **134**, 4509–4512.
32 S. Kuppuswamy, A. J. Peloquin, I. Ghiviriga, K. A. Abboud and A. S. Veige, *Organometallics*, 2010, **29**, 4227–4233.
33 S. Sarkar, A. R. Carlson, M. K. Veige, J. M. Falkowski, K. A. Abboud and A. S. Veige, *J. Am. Chem. Soc.*, 2008, **130**, 1116–1117.
34 C. D. Roland, H. Li, K. A. Abboud, K. B. Wagener and A. S. Veige, *Nat. Chem.*, 2016, **8**, 791–796.
35 P. T. Boeck, R. Yadav, B. S. Sumerlin and A. S. Veige, *Macromolecules*, 2024, **57**, 71–77.
36 H. R. Kricheldorf and S. R. Lee, *Macromolecules*, 1995, **28**, 6718–6725.
37 Y. A. Chang and R. M. Waymouth, *J. Polym. Sci., Part A: Polym. Chem.*, 2017, **55**, 2892–2902.
38 M. Ouchi, H. Kammiyada and M. Sawamoto, *Polym. Chem.*, 2017, **8**, 4970–4977.
39 B. A. Laurent and S. M. Grayson, *Chem. Soc. Rev.*, 2009, **38**, 2202–2213.
40 R. Tuba, *Pure Appl. Chem.*, 2014, **86**, 1685–1693.
41 M. Ahmad and S. M. Grayson, *Mass Spectrom. Rev.*, 2024, 1–29.
42 T. Kubo, R. Yadav and A. S. Veige, *Topological Polymer Chemistry: Concepts and Practices*, Springer Nature, 2022, pp. 261–275.
43 K. P. Mcgowan, M. E. O'Reilly, I. Ghiviriga, K. A. Abboud and A. S. Veige, *Chem. Sci.*, 2013, **4**, 1145–1155.
44 A. M. Esper, *PhD Thesis*, University of Florida, 2023.
45 C. D. Roland, T. Zhang, S. Venkatramani, I. Ghiviriga and A. S. Veige, *Chem. Commun.*, 2019, **55**, 13697–13700.
46 Z. Miao, D. Pal, W. Niu, T. Kubo, B. S. Sumerlin and A. S. Veige, *Macromolecules*, 2020, **53**, 7774–7782.
47 S. M. Holmes, D. F. Schafer, P. T. Wolczanski and E. B. Lobkovsky, *J. Am. Chem. Soc.*, 2001, **123**, 10571–10583.
48 T. W. Hayton, J. M. Boncella, B. L. Scott, K. A. Abboud and R. C. Mills, *Inorg. Chem.*, 2005, **44**, 9506–9517.
49 R. J. Beattie, P. S. White and J. L. Templeton, *Organometallics*, 2016, **35**, 32–38.
50 R. Yadav, I. Ghiviriga, K. K. Abboud and A. S. Veige, *Chem. Commun.*, 2023, **59**, 12899–12902.
51 A. W. Addison, T. N. Rao, J. Reedijk, J. van Rijn and G. C. Verschoor, *J. Chem. Soc., Dalton Trans.*, 1984, 1349–1356.
52 M. H. Chisholm, K. Folting, D. M. Hoffman, J. C. Huffman and J. Leonelli, *J. Chem. Soc., Chem. Commun.*, 1983, 589–591.
53 I. M. Bartlett, N. G. Connelly, M. S. Legge, A. J. Martin, B. Metz and A. G. Orpen, *Chem. Commun.*, 1996, **2**, 1877–1878.
54 L. J. Canoira, J. L. Davidson, G. Douglas and K. W. Muir, *J. Organomet. Chem.*, 1989, **362**, 135–146.
55 S. A. Gonsales, T. Kubo, M. K. Flint, K. A. Abboud, B. S. Sumerlin and A. S. Veige, *J. Am. Chem. Soc.*, 2016, **138**, 4996–4999.
56 S. S. Nadif, T. Kubo, S. A. Gonsales, S. Venkatramani, I. Ghiviriga, B. S. Sumerlin and A. S. Veige, *J. Am. Chem. Soc.*, 2016, **138**, 6408–6411.
57 V. K. Jakhar, A. M. Esper, I. Ghiviriga, K. A. Abboud, C. Ehm and A. S. Veige, *Angew. Chem., Int. Ed.*, 2022, **61**, e202203073.

58 V. Jakhar, D. Pal, I. Ghiviriga, K. A. Abboud, D. W. Lester, B. S. Sumerlin and A. S. Veige, *J. Am. Chem. Soc.*, 2021, **143**, 1235–1246.
59 R. Yadav, A. M. Esper, I. Ghiviriga, K. A. Abboud, W. Lester, C. Ehm and A. S. Veige, *ChemCatChem*, 2024, e202301678.
60 R. D. Bach, *J. Am. Chem. Soc.*, 2009, **131**, 5233–5243.
61 T. Harris and I. V. Alabugin, *Mendeleev Commun.*, 2019, **29**, 237–248.
62 N. J. Agard, J. A. Prescher and C. R. Bertozzi, *J. Am. Chem. Soc.*, 2004, **126**, 15046–15047.
63 G. De Almeida, E. M. Sletten, H. Nakamura, K. K. Palaniappan and C. R. Bertozzi, *Angew. Chem., Int. Ed.*, 2012, **51**, 2443–2447.
64 T. J. Katz and S. J. Lee, *J. Am. Chem. Soc.*, 1980, **102**, 422–424.
65 K. Yamada, R. Nomura and T. Masuda, *Macromolecules*, 2000, **33**, 9179–9181.
66 P. Mastrorilli, F. Nobile, A. Rizzuti, G. P. Suranna, D. Acierno and E. Amendola, *J. Mol. Catal. A: Chem.*, 2002, **178**, 35–42.
67 O. Trhlíková, J. Zedník, H. Balcar, J. Brus and J. Sedláček, *J. Mol. Catal. A: Chem.*, 2013, **378**, 57–66.
68 C. W. Bielawski, D. Benitez and R. H. Grubbs, *Science*, 2002, **297**, 2041–2044.
69 W. Niu, S. A. Gonsales, T. Kubo, K. C. Bentz, D. Pal, D. A. Savin, B. S. Sumerlin and A. S. Veige, *Chem*, 2019, **5**, 237–244.
70 Z. Miao, T. Kubo, D. Pal, B. S. Sumerlin and A. S. Veige, *Macromolecules*, 2019, **52**, 6260–6265.
71 J. N. Hoskins and S. M. Grayson, *Polym. Chem.*, 2011, **2**, 289–299.